Faraday Discussions

Accepted Manuscript

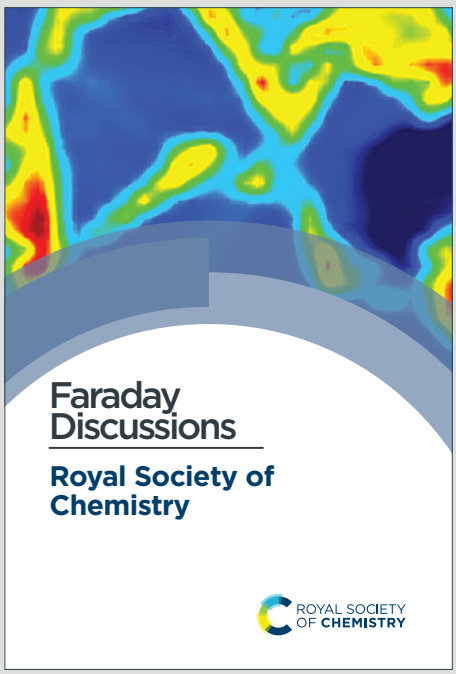

This article can be cited before page numbers have been issued, to do this please use: L. Liu, *Faraday Discuss.*, 2024, DOI: 10.1039/D4FD00147H.

ROYAL SOCIETY OF CHEMISTRY

www.rsc.org/faraday_d

View Article Online
DOI: 10.1039/D4FD00147H

ARTICLE

Charge induced deformation of scanning electrolyte before contact

Received 00th January 20xx,
Accepted 00th January 20xx

DOI: 10.1039/x0xx00000x

Liang Liu*

The recent developments of scanning electrochemical probe techniques focus on the strategy of scanning electrolyte. For example, scanning electrochemical cell microscopy (SECCM) is based on holding the electrolyte in a glass capillary, while scanning gel electrochemical microscopy (SGECM) immobilizes the gel electrolyte on micro-disk electrodes or etched metal wires. In both SECCM and SGECM, the first and essential step is to approach the electrolyte probe to be in contact with the sample, which is very often achieved by current feedback with a constant applied potential between the probe and the sample. This work attempts to theoretically analyse the deformation of electrolyte during this approaching process. For liquid electrolyte in SECCM, surface tension is considered to counterbalance the gravity and electrostatic force in 2D cylindrical coordinates with axial symmetry. The deformation at equilibrium is solved under certain conditions. For gel electrolyte, a viscoelastic gel is analysed with simplified 1D geometry. Both equilibrium and dynamic approaching are considered. The results suggest that for both liquid and gel electrolytes, critical conditions exist for breaking the equilibrium. When applied potential is higher or the distance is lower than the threshold, the force will not equilibrate and the electrolyte will deform until contact. The critical condition depends on the properties (surface tension for liquid, elastic and viscous modulus for gel) and geometry (radius of capillary for liquid, thickness for gel) of electrolyte. Prospects of further extending the work closer to real experimental scenarios, especially SGECM, are also discussed.

Introduction

Scanning electrochemical probe techniques are powerful tools for studying spatially localized electrochemistry. The most well-known concept is based on scanning a micro- or nano- electrode that is positioned close to the sample immersed in electrolyte. This includes scanning electrochemical microscopy and scanning ion conductance microscopy, both being developed since the end of 1980s[1,2]. So far, they have been successfully used in electrochemical imaging and patterning by localizing various electrochemical reactions[3].

Recently, another strategy of scanning the electrolyte instead of the electrode is attracting arising interest. This was initially referred as scanning droplet cell[4–7], or electrochemical pen[8,9], and now is more commonly accepted as scanning electrochemical cell microscopy (SECCM)[10–13]. It is based on holding the electrolyte in a pulled capillary, then approaching the capillary close to the sample so that the electrolyte can wet the sample surface which bridges the electrical circuit for measure. The origin of the concept may even date back to 1970s and 1980s, when researchers used nozzles that are placed close to the substrate and applied a jet flow for electrohydrodynamic printing[14–18].

The success of SECCM relies on pushing the spatial resolution of scanning electrochemical probe techniques into nanoscale without sophisticated probe fabrication, thanks to the matured protocol of pulling glass capillaries which was already widely used in electro-physiology measurements[11]. The liquid trace after the measurement also indicates the area of measurement, which allows correlation with other ex-situ characterizations for getting comprehensive structure-reactivity relationship of the material[19]. Nevertheless, in terms of quantification, the wetting of electrolyte on the surface, which is essential for the measurement but not easy to control and may depend on the surface hydrophobicity and local roughness, will affect the analysis. Experimentally, various effort has been made to address this issue, such as regulating the contact by immersing the sample in oil[20,21] or observation of the contact with interference reference microscopy[22]. From the analysis aspect, 2D (for single cylindrical capillary) or 3D (for multi-barrelled capillary) models are required for deriving the charge transfer kinetics in the contact area taking the geometry of droplet into consideration.

Meanwhile, it is proven that the immobilization of electrolyte in the form of gel may inhibit the wetting of electrolyte on the electrode surface, while still keeping the localized contact. It can be achieved by filling the capillary with gel[23–26], or by electrodeposition of gel on micro-disk electrodes or sharpened metal wires[27–30]. The latter get rid of the capillary, and is denoted as scanning gel electrochemical microscopy (SGECM). It is shown that SGECM may greatly inhibit the wetting of electrolyte over the sample surface[31]. The elasticity of the gel

[a] Laboratoire de Chimie Physique et Microbiologie pour les Matériaux et l'Environnement (LCPME), Universite de Lorraine, CNRS, Nancy 54000, France
*Email : liang.liu@cnrs.fr

Supplementary Information available: Explanation of dynamic grid for conformal map and Matlab codes for the results. See DOI: 10.1039/x0xx00000x

allows tuning the contact area by pressing or retracting the probe, which brings an advantage of flexible spatial resolution but also complicates the quantitative analysis due to the moving boundary[29].

The experiments of SECCM and SGECM generally follow the same protocol[11,27–29]. The first step is to approach the probe of electrolyte (either in liquid or in gel form) to be in contact with the sample surface. Then, electrochemical measurements are carried out, with only limited area of the sample exposed to the electrolyte. For lateral scans, the probe is retracted from the sample until fully detached, then it is laterally moved to the next sampling point before re-executing the first step. Such loop of intermittent contact allows constructing the map of electrochemical reactivity, while ensuring that each pixel is measured independently.

The most straightforward way to sense the contact between the electrolyte probe and the sample surface is by current feedback. By applying potential between the probe and the sample, a current spike will turn up upon their contact due to the bridging of the circuit. This signal is highly useful for the instrumentation, while the electrochemistry is usually analysed "later" (in the order of milliseconds) by measuring from the probe on hold. Here, a question arises out of curiosity: What is the physical meaning of this current at very first contact? It is usually discarded for analysis due to the complexity, which at least consists of electrical discharging and non-Faradaic behaviour. However, it may help understanding the formation of solid-electrolyte interface at the very beginning of electrode-electrolyte contact. Then another question arises: Is the electrolyte still like the free form at the moment of contact?

In this work, we will address the latter question by deriving the deformation of electrolyte under electric field before contact in SECCM and SGECM. As a preliminary work, only equilibrium state is considered for SECCM, where the surface tension is balanced with electrical force and gravity at the electrolyte boundary. The results indicate the presence of critical conditions, beyond which the equilibrium cannot be maintained until the electrolyte wets the sample. For the gel electrolyte, a simple gel film on planar electrode is considered so that the system can be analysed in 1D. Even though it is far from the experimental reality in SGECM, it eases the mathematical treatment and allows exploring the dynamic behaviour considering the viscoelasticity of the gel. Similar as liquid electrolyte, the critical condition of breaking equilibrium also exists, which can be proven mathematically. For dynamic behaviour, the approaching speed will affect the state of stretching of gel upon contact with the sample.

Deformation of liquid electrolyte in SECCM

The problem of deformation of liquid under electric field has been intensively studied in 1970s following the inauguring work of Taylor[32–35]. The main interest was to better understand and control the electrohydrodynamic deposition, such as electrospinning and electrospraying. These works mainly consider highly resistive dielectric liquid, and the electric field was usually considered homogeneous to neglect the geometric effect. With the later development of numerical methods, some open source tools were also developed to simulate these processes, such as JetSpin[36].

Different from the cases above, spatially localized electrochemical measurements usually involve well supported electrolyte that is highly conductive. Moreover, the potential applied on the electrolyte (through the counter electrode) *versus* the sample (electric ground) is usually less than 1.5 V, for the consideration of not initiating violent reactions (*e.g.* electrolysis of water) upon contact. These make it reasonable to neglect the potential drop in the electrolyte so that the whole electrolyte can be regarded as an equipotential body.

In experimental practice of SECCM, the inner wall of the capillary is usually treated to be hydrophilic, while the outer wall is treated to be hydrophobic. Therefore, we may assume that the friction between the liquid electrolyte and the inner wall is negligible, and the outer wall of the capillary is infinitely repellant so that the liquid electrolyte will never spread on it. Taking these approximations and considering that the sample is connected to the ground, the problem can be described in **Scheme 1**.

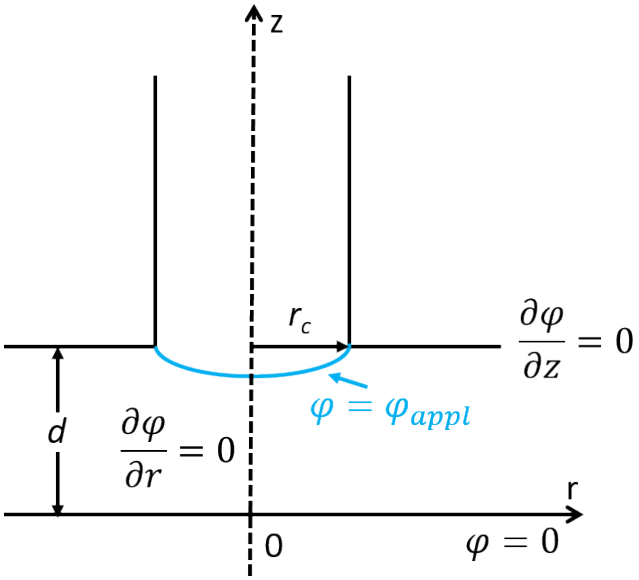

Scheme 1. Illustration of liquid electrolyte out of glass capillary in SECCM with boundary conditions.

At equilibrium state, the governing equation of pressure balance shall be expressed as:

$\Delta p_{surf} + p_g + p_e = 0$ (*Eq.* 1)

where p_{surf} represents the pressure induced by surface tension of liquid electrolyte, p_g represents the pressure from gravity, and p_e refers to the pressure induced by electric field. p_{surf} follows Young-Laplace Equation:

$\Delta p_{surf} = -2\gamma H$ (*Eq.* 2)

where γ is the surface tension of electrolyte and H is the mean curvature of the electrolyte boundary. p_g can be expressed as:

$p_g = \rho g h$ (*Eq.* 3)

where ρ is the density of electrolyte, g is gravitation acceleration, h is the height of electrolyte in the capillary. In this work, we always consider $\rho = 1 \times 10^3$ kg/m^3, $g = 9.8$ m/s^2 and $h = 5 \times 10^{-2}$ m. One may see later that in most cases the pressure of gravity is negligible as compared with surface tension and electric terms, especially for capillaries with nanometer size radius. p_e is the pressure induced by electrical force, which depends on the electric field at the electrolyte boundary:

$p_e = \varepsilon\varepsilon_0\left(\overrightarrow{E_{curv}} \cdot \vec{n}\right)^2$ (*Eq.* 4)

ε_0 is the vacuum permittivity, with value of 8.85×10^{-12} F·m^{-1}. ε is the dielectric constant of the media between the electrolyte and the sample, which is approximately 1 for air thus neglected in this work.

E_{curv} is the electric field vector with unit V/m, and *n* is the unit normal vector, both at the boundary of electrolyte.

The electric field can be solved from Laplace Equation expressed in cylindrical coordinates with axial symmetry in *z*:

$\frac{\partial^2\varphi}{\partial r^2}+\frac{1}{r}\frac{\partial\varphi}{\partial r}+\frac{\partial^2\varphi}{\partial z^2}=0$ (*Eq.* 5)

The boundary conditions are as follows:

$r=0, \frac{\partial\varphi}{\partial r}=0$ (*Eq.* 6)

$r=\infty, \varphi=0$ (*Eq.* 7)

$z=0, \varphi=0$ (*Eq.* 8)

$z=d$ and $r\in(r_c,\infty), \frac{\partial\varphi}{\partial r}=0$ (*Eq.* 9)

Denote the electrolyte boundary as $z=f(r)$, then

$z=f(r), \varphi=0$ (*Eq.* 10)

The expression of $f(r)$ is what we need to solve, so that the pressure balance is fulfilled for equilibrium state. Or in another word, if $f(r)$ is known, *Eq.* 5 can be solved with boundary conditions *Eqs.* 6-10, and then the electric pressure term can be calculated from *Eq.* 4.

For the ease of numerical treatment, the distance can be normalized to r_c and the potential can be normalized to the applied potential φ_{appl}:

$R=\frac{r}{r_c}$ (*Eq.* 11)

$Z=\frac{z}{r_c}$ (*Eq.* 12)

$\phi=\frac{\varphi}{\varphi_{appl}}$ (*Eq.* 13)

The algorithm for solving $f(R)$ starts from an initial value, denoted as $f_{old}(R)$. Based on this, the potential gradient $\Phi(R,Z)$ can be solved, and p_e can be calculated. Then, the new curve of electrolyte boundary, denoted as $f_{new}(r)$, can be calculated from the potential balance and the expression of curvature:

$\frac{f''_{new}(R)}{(1+f'^2_{new}(R))^{\frac{3}{2}}}=\frac{\frac{\varepsilon_0\varphi_{appl}^2}{r_c^2}E_n^2+\rho g h}{\frac{2\gamma}{r_c}}\equiv g(R)$ (*Eq.* 14)

E_n is the dimensionless electric field that is normal to the electrolyte boundary, which is a scalar and can be numerically obtained from the gradient of ϕ (dimensionless vector) and the unit normal vector at each *R*. Thus, the right side of the equation is denoted as a dimensionless function $g(R)$.

With the symmetry boundary condition:

$R=0, f'_{new}(R)=0$ (*Eq.* 15)

The equation above can be solved by integrating both sides:

$\frac{f'_{new}(R)}{(1+f'^2_{new}(R))^{\frac{1}{2}}}=\int_0^R g(R)dR\equiv G(R)$ (*Eq.* 16)

$f'_{new}(R)=\sqrt{\frac{G(R)^2}{1-G(R)^2}}$ (*Eq.* 17)

Knowing $f'_{new}(R)$, $f_{new}(R)$ can be derived with the boundary condition:

$f_{new}(1)=\frac{d}{r_c}$ (*Eq.* 18)

The loop will continue until convergence $f_{new}(R)=f_{old}(R)$.

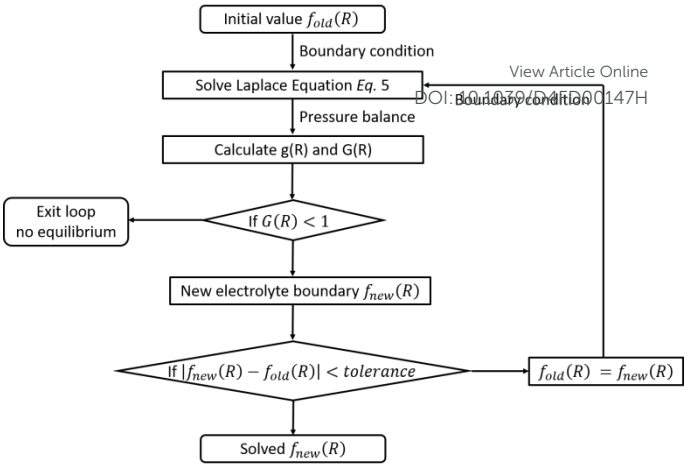

Scheme 2. Algorithm of iterating *f(R)* until convergence or breaking the equilibrium.

Note that for each iteration, one has to solve Laplace Equation with a new boundary. This is achieved efficiently by ADI method using dynamic grid based on conformal map[37], as detailed in Supporting Information.

Figure 1 shows the evolution of the electrolyte boundary as a result of applying different potential, fixing the capillary at 100 nm above the sample. For a capillary with radius 1 μm (**Figure 1A**), it is seen that even 0.5 V may induce visible deformation, while at 3 V the electrolyte is heavily deformed with the tip close to the sample. In contrast, a thinner capillary with radius 0.1 μm shows much less deformation upon applying potential (**Figure 1B**). The deformation is almost invisible when the applied potential is up to 5 V. Even by applying 10 V, the deformation is still less than that corresponds to 3 V in **Figure 1A**. This is because for the same extent of deformation (measured by the displacement at *r* = 0), the surface tension is much higher for thinner capillaries, thus may counterbalance a larger force from higher electric field. It suggests that by reducing the diameter of the capillary, one may not only gain the lateral spatial resolution but also gain the vertical precision of approaching the probe in SECCM. Similarly, it is not difficult to expect less deformation by using an electrolyte of higher surface tension, although in experimental practice it may bring difficulties in filling into the thin capillaries.

DOI: 10.1039/D4FD00147H

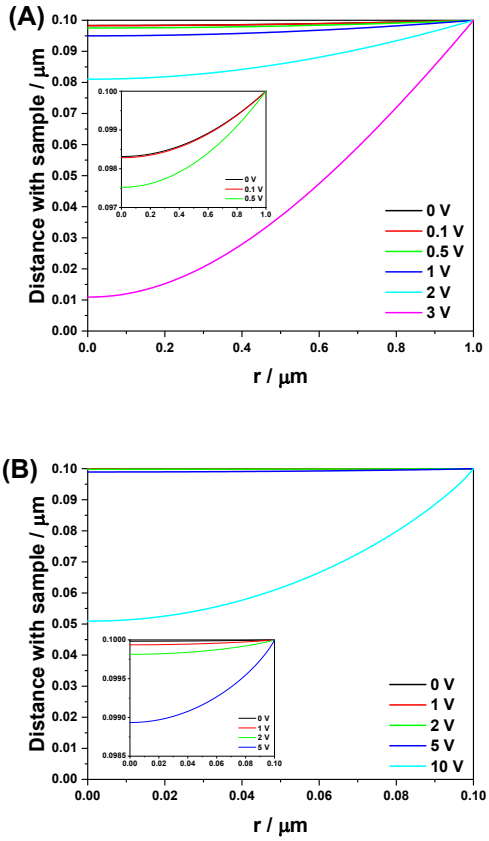

Figure 1. The deformation of electrolyte under different applied potential: (A) r_c = 1 μm; (B) r_c = 100 nm.

It should be noted that no convergent solution was obtained by applying higher potential in **Figure 1**. The can be explained by the physical meaning of the algorithm (**Scheme 2**). The initial value corresponds to the equilibrium state of the electrolyte boundary without electric field. Then, potential is applied between the electrolyte and the sample inducing the deformation of electrolyte boundary. The latter reduces the distance between the electrolyte and the sample (electrolyte falling out of the capillary). Qualitatively, it will always increase the intensity of electric field thus increase p_e, yet it may not be always fully compensated by the change of p_{surf}. That is to say, it may exist a critical condition that breaks the equilibrium, similar to the formation of Taylor cone.

The critical condition can be obtained from the validity of *Eq.* 17 in order that $f'_{new}(R)$ being real:

$G(R) < 1$ (*Eq.* 19)

From *Eq.* 14 it is seen that for a given system, the only variables for $G(R)$ are φ_{appl} and E_n, while the latter is dependent on the normalized distance between the capillary and the sample d/r_c. Mathematically and physically, it is not difficult to envisage that the equilibrium may be broken if φ_{appl} is higher than a critical value for a fixed *d*, or if *d* is lower than a critical value for a fixed φ_{appl}. More rigorous derivations may be carried out by looking at the dynamic deformation of electrolyte in future.

The critical values were calculated numerically by searching the critical point of breaking the convergence, with the criteria of *Eq.* 19 **Figure 2** shows the effect of capillary size on the critical potential, with the probe-sample distance *d* in the range of 1 to 100 nm. It is seen that as the radius of capillary increases, the critical potential decreases. This agrees with the trend in **Figure 1**, where the deformation of liquid electrolyte in larger capillaries is more sensitive to the applied potential.

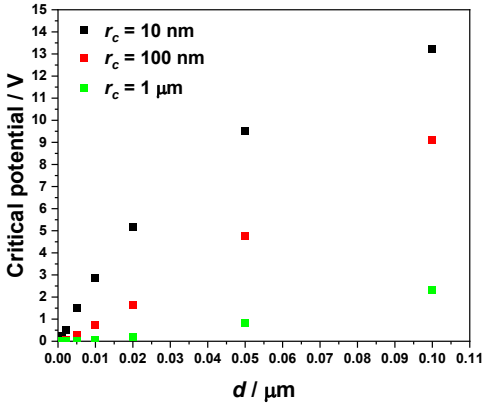

Figure 2. The critical potential at different *d* for capillaries of different radius.

A simplified scenario of deformation of gel electrolyte

In SGECM, the geometry of gel probe is not straightforward as it depends on the pH profile during the electrodeposition (+ pulling) process for both Type I and Type II probes[30,38]. The deformation of such shapes is not easy to treat. Here, as a preliminary effort to look into the problem, we leave aside the geometrical effect and try to study a simplified case in 1D. The advantage is that the solutions will be analytical with clear physical meaning. It will help understanding the physics and can be extended to higher dimensions in future work. Note that such treatment is difficult to implement for liquid electrolyte as the liquid cannot stand alone without support.

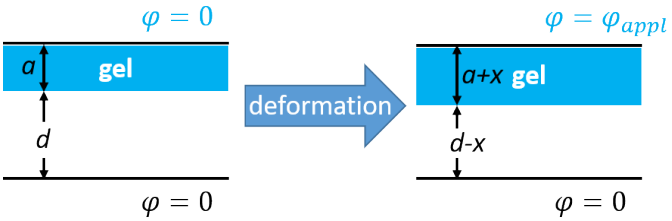

Scheme 3. Illustration of gel electrolyte in 1D.

Consider a planar gel electrode that is placed in parallel to a planar solid sample with a distance *d*. The gel electrolyte film has thickness *a* at free form, as illustrated in **Scheme 3**. Applying the same approximation of well supported gel electrolyte so that φ_{appl} is homogeneously applied on it, the gel will be stretched due to the electrostatic force. If the gel is deformed by *x* as a result of electric field, the stress-strain relationship can be expressed by Hooke's Law assuming that the gel is a linear elastic body:

$\frac{\varepsilon_0 \varphi_{appl}^2}{(d-x)^2} = E_Y \frac{x}{a}$ (*Eq.* 20)

where E_Y is the elastic modulus of the gel. The equation can be reorganized as follows:

$\frac{\varepsilon_0 \varphi_{appl}^2 a}{E_Y} = x(d-x)^2$ (*Eq.* 21)

For $x \in [0,d]$, the right side has a maximum value of $\frac{4}{27}d^3$ at $x = \frac{1}{3}d$. That is to say, if

$\frac{\varepsilon_0 \varphi_{appl}^2 a}{E_Y} > \frac{4}{27}d^3$ (*Eq.* 22)

the equilibrium is impossible and the gel will be stretched until touching the sample. Taking an example of a = 10 μm and E_Y = 10 kPa, **Figure 3** illustrates the trend of critical potential as a function of distance. It is seen that the critical potential increases as the distance increases. Assume φ_{appl} = 1 V, the critical distance is 3.9×10^{-7} m, that is to say, one may not approach the gel probe closer than this distance to the sample. According to *Eq.* 22 the critical distance can be reduced by reducing the thickness or increasing the elastic modulus of gel.

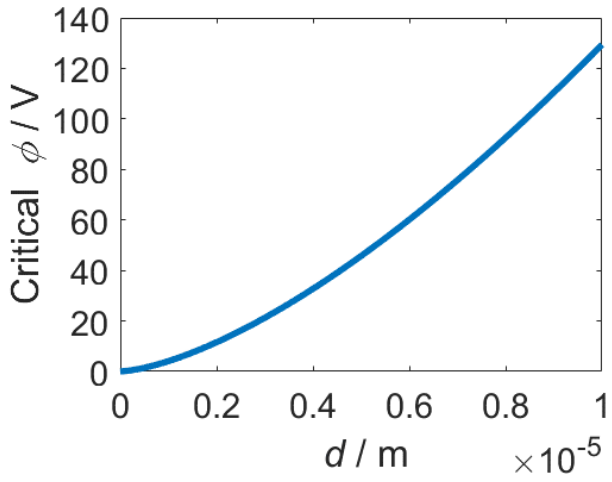

Figure 3. Critical potential as a function of distance for 1D gel film of thickness 10 μm and elastic modulus 10 kPa.

The results above prove the existence of critical condition of contact, which depends on the applied potential on the probe and the gel properties, *i.e.* elastic modulus and thickness. In general, the applied potential makes the contact occurring earlier when approaching the probe. For a given gel probe and a fixed potential for approaching the probe, all these parameters are presumably constant so that the touching position can still be used for constructing the topography of the sample. However, one should be aware of the possible artefacts even though the 1D oversimplification here is not the same as the experimental practice in SGECM.

The existence of critical condition of contact, or the break of equilibrium state, is similar as the case of liquid electrolyte. The only difference is that the force for retaining the shape of liquid electrolyte is surface tension, while that for gel electrolyte is elasticity.

The oversimplification of gel electrolyte in 1D offers a huge advantage for the ease of mathematical treatment, which allows exploring the dynamic behaviour of the gel during approaching. Here, we consider that the gel probe is approaching the sample at a constant potential φ_{appl} and constant speed v, and the gel is viscoelastic following Kelvin-Voigt model. The stress-strain relationship in *Eq.* 20 can be replaced by:

$\frac{\varepsilon_0 \varphi_{appl}^2}{(d-vt-x)^2} = E_Y \frac{x}{a} + \frac{\eta}{a}\frac{dx}{dt}$ (*Eq.* 23)

where η is the viscous modulus of the gel in unit Pa·s. Denote $X = \frac{x}{a}$ and $d_n = \frac{x}{a}$ in dimensionless form, and $v_n = \frac{v}{a}$ with unit s^{-1}, the equation above can be rewritten as:

View Article Online DOI: 10.1039/D4FD00147H

$\frac{dX}{dt} = \frac{\varepsilon_0 \varphi_{appl}^2}{a^2 \eta (d_n - v_n t - X)^2} - \frac{E_Y}{\eta} X$ (*Eq.* 24)

It can be solved implicitly with initial condition X = 0 at t = 0.

One may further derive the current density. At any t, the areal capacitance C_a in unit $F \cdot m^{-2}$ can be expressed as:

$C_a = \frac{\varepsilon_0}{a(d_n - v_n t - X)}$ (*Eq.* 25)

With the constant potential φ_{appl}, the current density can be expressed as:

$i = \varphi_{appl} \frac{dC_a}{dt} = \frac{\varepsilon_0 \varphi_{appl}}{a} \frac{1}{(d_n - v_n t - X)^2} \frac{dX}{dt}$ (*Eq.* 26)

Knowing the solution of $X(t)$ from *Eq.* 24 the current can also be derived.

Figure 4 shows an example where a gel probe with thickness 10 μm is approached to the sample at a speed of 1 μm/s, under a constant potential 1 V. The probe is initially positioned at 20 μm away from the sample. Instead of 20 s, the probe runs into contact with the sample at only 19.73 s, and the gel is stretched by 0.28 μm upon contact. Meanwhile, the current shows a spike upon contact, which is similar as experimental observations. From the magnified image (right), it is seen that the current starts to increase when the sample-probe distance starts to sharply decrease. In experimental practice, the probe will stop approaching when the current reaches an arbitrarily set threshold (usually higher than noise). Yet, if the Eq. is met, the gel will continue stretching until touching the sample.

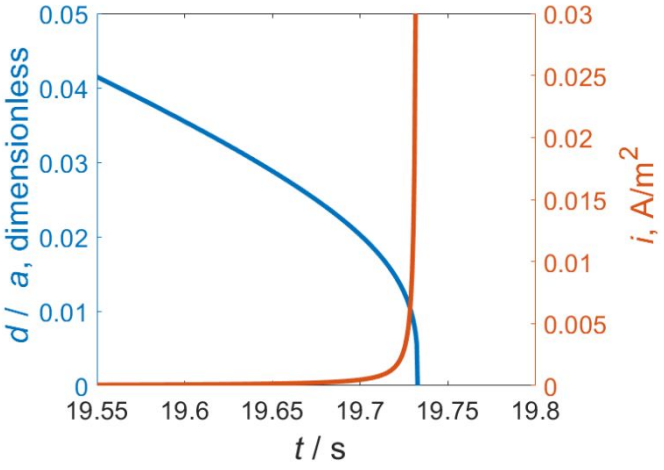

Figure 4. Example of gel probe with thickness a = 10 μm approaching at v = 1 μm/s under constant potential φ_{appl} = 1 V. E_Y = 10 kPa, η = 1 kPa·s. (Only showing the zone close to contact).

Figure 5 shows the effect of approaching speed on the contact behaviour. It is interesting to see that the probe will stop at different position, *i.e.* with different stretching, with different approaching speed. The slower the approaching is, the closer the system is to the pure elastic behaviour, and the more the gel is stretched at contact. Apart from the approaching speed, the applied potential φ_{appl}, the gel thickness a, the elastic modulus E_Y and the viscous modulus η will also affect the contact. The readers may use the code in supporting information to calculate. Note that although the 1D system is oversimplified as compared with the experimental scenarios, one should still be careful with the current feedback in SGECM. It is

recommended to keep the same approaching speed for the same probe so that the contact position will not vary in the same experiment.

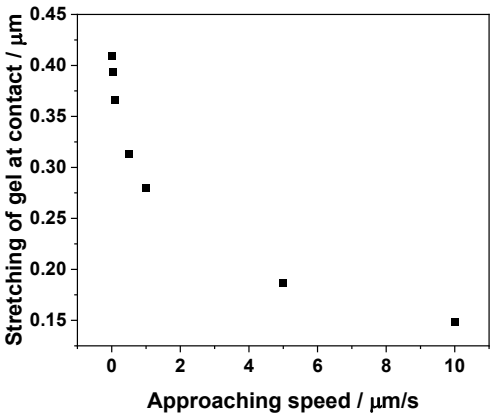

Figure 5. Effect of approaching speed on the stretching of gel at contact. a = 10 μm, φ_{appl} = 1 V, E_Y = 10 kPa, η = 1 kPa·s.

It should be noted that the parameters in this work are selected arbitrarily within reasonable range, especially for the gel properties. For the specific experimental systems, the readers may adapt and calculate using the code provided in Supporting Information.

Summary and prospects

In summary, the deformation of electrolyte when approaching the liquid or gel probe to the sample in SECCM and SGECM is preliminarily analyzed theoretically. The problem is turned into the pressure balance among surface tension for liquid or viscoelasticity for gel, electrostatic force from the electric field and gravity (although usually negligible for nanometer sized capillaries). For liquid electrolyte, the system is analyzed at equilibrium in 2D cylindrical coordinates with axial symmetry. For any fixed distance from the sample, the deformed electrolyte boundary under applied potential is solved numerically. It is important to note that the equilibrium state is not always valid. When the applied potential exceeds a threshold for a fixed distance, or when the distance is smaller than a threshold for a fixed applied potential, the equilibrium may be broken and the electrolyte will deform until wetting the sample. The critical condition depends on the radius of the capillary as well as the surface tension of the liquid. For gel electrolyte, the system is first simplified to 1D considering a viscoelastic gel. A critical condition is also seen for the equilibrium state, which depends on the thickness and elastic modulus of the gel. Moreover, dynamic approaching shows that the touching position depends on the approaching speed, which is attributed to the viscoelastic effect. In general, critical condition of equilibrium exists for both liquid and gel electrolyte, and it depends on the properties (surface tension for liquid, elastic and viscous modulus for gel) and geometry (radius of capillary for liquid, thickness for gel) of the electrolyte.

This preliminary work offers better understanding of the approaching behaviour of probes in SECCM and SGECM. Further work may target at dynamic deformation of liquid electrolyte. For liquid with negligible viscosity, Bernoulli Equation can be used so that the pressure difference at the liquid boundary is converted to a velocity term. For viscous liquid, Navier-Stokes Equations shall be considered to solve the velocity distribution. This is expected to rigorously reveal the system behaviour regardless of the existence of equilibrium. For the gel electrolyte, the geometry of the gel shall be considered and the elastic deformation can be solved from Navier-Cauchy Equation. It is also interesting to compare with experimental results, especially by *in-situ* monitoring of the shape of electrolyte with IRM[22]. However, one shall pay attention to the measurement of the initial current at the moment of contact (t = 0), as it is challenging for instrumentation due to the background noise, the limited bandwidth, and the response time for feedback.

View Article Online DOI: 10.1039/D4FD00147H

Conflicts of interest

There are no conflicts to declare.

Data availability

The data supporting this work, including the source code in Matlab, is included in the Supporting information.

Acknowledgements

This work is supported by ANR-NRF project MEACT (ANR-20-CE09-0028). The author also acknowledges Paul Roger, student from ENS Lyon, for constructive discussions on the work.

References

1 A. J. Bard, F. R. F. Fan, J. Kwak and O. Lev, *Anal Chem*, 1989, **61**, 132–138.
2 P. K. Hansma, B. Drake, O. Marti, S. A. C. Gould and C. B. Prater, *Science*, 1989, **243**, 641–643.
3 A. J. Bard and M. V. Mirkin, *Scanning Electrochemical Microscopy*, CRC Press, Boca Raton, 2022.
4 J. D. Madden and I. W. Hunter, *Journal of Microelectromechanical Systems*, 1996, **5**, 24–32.
5 M. M. Lohrengel, *Electrochim Acta*, 1997, **42**, 3265–3271.
6 A. W. Hassel and M. M. Lohrengel, *Electrochim Acta*, 1997, **42**, 3327–3333.
7 M. M. Lohrengel, A. Moehring and M. Pilaski, *Fresenius J Anal Chem*, 2000, **367**, 334–339.
8 F. Cortés-Salazar, A. Lesch, D. Momotenko, J. M. Busnel, G. Wittstock and H. H. Girault, *Analytical Methods*, 2010, **2**, 817–823.
9 A. P. Suryavanshi and M.-F. Yu, *Nanotechnology*, 2007, **18**, 105305.
10 M. E. Snowden, A. G. Güell, S. C. S. Lai, K. McKelvey, N. Ebejer, M. A. Oconnell, A. W. Colburn and P. R. Unwin, *Anal Chem*, 2012, **84**, 2483–2491.
11 G. Jayamaha, M. Maleki, C. L. Bentley and M. Kang, *Analyst*, 2024, 149, 2542–2555.
12 L. F. Gaudin, I. R. Wright, T. R. Harris-Lee, G. Jayamaha, M. Kang and C. L. Bentley, *Nanoscale*, 2024, **16**, 12345–12367.
13 N. Ebejer, A. G. Güell, S. C. S. Lai, K. McKelvey, M. E. Snowden and P. R. Unwin, *Annual Review of Analytical Chemistry*, 2013, **6**, 329–351.
14 R. C. Alkire and T. Chen, *J Electrochem Soc*, 1982, **129**, 2424–2432.

View Article Online
DOI: 10.1039/D4FD00147H

15 J. D. Whitaker, J. B. Nelson and D. T. Schwartz, *Journal of Micromechanics and Microengineering*, 2005, **15**, 1498–1503.
16 B. W. An, K. Kim, H. Lee, S. Y. Kim, Y. Shim, D. Y. Lee, J. Y. Song and J. U. Park, *Advanced Materials*, 2015, **27**, 4322–4328.
17 J. He, F. Xu, Y. Cao, Y. Liu and D. Li, *J Phys D Appl Phys*, 2016, **49**, 055504.
18 G. Olivier, Scanning nozzle plating system, US Patent 3810829, 1974.
19 O. J. Wahab, M. Kang and P. R. Unwin, *Curr Opin Electrochem*, 2020, **22**, 120–128.
20 E. Daviddi, V. Shkirskiy, P. M. Kirkman, M. P. Robin, C. L. Bentley and P. R. Unwin, *Chem Sci*, 2021, **12**, 3055–3069.
21 Y. Li, A. Morel, D. Gallant and J. Mauzeroll, *Anal Chem*, 2020, **92**, 12415–12422.
22 D. Valavanis, P. Ciocci, G. N. Meloni, P. Morris, J. F. Lemineur, I. J. McPherson, F. Kanoufi and P. R. Unwin, *Faraday Discuss*, 2021, **233**, 122–148.
23 Y. Takahashi, T. Yamashita, D. Takamatsu, A. Kumatani and T. Fukuma, *Chemical Communications*, 2020, **56**, 9324–9327.
24 M. E. Snowden, M. Dayeh, N. A. Payne, S. Gervais, J. Mauzeroll and S. B. Schougaard, *J Power Sources*, 2016, **325**, 682–689.
25 M. Kang, P. Wilson, L. Meng, D. Perry, A. Basile and P. R. Unwin, *Chemical Communications*, 2018, **54**, 3053–3056.
26 M. Donnici and S. Daniele, *Journal of Solid State Electrochemistry*, 2020, **24**, 2861–2869.
27 L. Liu, M. Etienne and A. Walcarius, *Anal Chem*, 2018, **90**, 8889–8895.
28 N. Dang, M. Etienne, A. Walcarius and L. Liu, *Electrochem commun*, 2018, **97**, 64–67.
29 N. Dang, M. Etienne, A. Walcarius and L. Liu, *Anal Chem*, 2020, **92**, 6415–6422.
30 M. A. Brites Helú and L. Liu, *Chemical Engineering Journal*, 2021, **416**, 129029.
31 G. A. Echeveste Salazar, M. A. Brites Helú, A. Walcarius and L. Liu, *Electrochim Acta*, 2023, **437**, 141455.
32 D. A. Saville, *Annu Rev Fluid Mech*, 1997, **29**, 27–64.
33 G. Taylor, *Proc R Soc Lond A Math Phys Sci*, 1964, **280**, 383–397.
34 S. Torza, R. G. Cox and S. G. Mason, *Philosophical Transactions of the Royal Society of London. Series A, Mathematical and Physical Sciences*, 1971, **269**, 295–319.
35 J. Hua, L. K. Lim and C.-H. Wang, *Physics of Fluids*, 2008, **20**, 113302.
36 M. Lauricella, G. Pontrelli, I. Coluzza, D. Pisignano and S. Succi, *Comput Phys Commun*, 2015, **197**, 227–238.
37 A. C. Michael, R. M. Wightman and C. A. Amatore, *J Electroanal Chem Interfacial Electrochem*, 1989, **267**, 33–45.
38 N. Dang, G. A. Echeveste Salazar, A. Walcarius and L. Liu, *Electrochim Acta*, 2024, **477**, 143753.

The Matlab code supporting this article have been included as part of the Supplementary Information.

View Article Online
DOI: 10.1039/D4FD00147H